

Versatile high-temperature high-pressure vapor cell design for electron beam excited laser studies

G. Marowsky, R. Cordray, F. K. Tittel, and W. L. Wilson

The design of a cell suitable for studying electron beam excited laser candidates at high temperatures such as organic dye and metal vapors is described. The cell is capable of handling temperatures up to 450°C and pressures from 10^{-6} Torr to 15 atm. Details of both the high-temperature laser performance of Ar-N₂ and the gain characteristics of the dye POPOP [2,2' phenylenebis(5-phenyloxazole)] are presented as an example of the use of such a cell.

I. Introduction

New electron beam excited laser systems, especially vapors of organic and inorganic materials, have aroused considerable interest in recent years.¹⁻⁶ Studies of these systems require both the electron beam technology developed for the successful operation of excimer lasers^{5,7} and a cell assembly capable of achieving appropriate vapor pressures of the potential active medium at elevated temperatures while permitting efficient electron beam deposition into a suitable dense buffer gas. For laser operation, a compact intracell optical resonator is needed to avoid optical losses due to the cell windows and to insure maximum electron beam interaction time in the active medium. This paper describes the design of such a high-temperature high-pressure cell assembly, a prealigned quartz optical resonator, and a procedure for characterizing and optimizing the electron beam diode configuration for this cell. A technique for measuring optical gain and some high-temperature measurements of gain in Ar-N₂ and argon buffered dye vapor mixtures using such a cell will also be presented.

II. Cell Description

The cell assembly is depicted in Fig. 1, showing (a) the reaction cell, (b) the optical resonator, (c) the anode foil, (d) the graphite cathode, (e) the optical cell window, (f) the gas handling system, and (g) the adaptor flange for

mounting the cell to the diode assembly of an electron beam generator. A cross-sectional view of the cell assembly and the field emission diode of a Physics International Pulserad 110 electron beam generator are shown in Fig. 2(a). The all stainless steel cell is designed to operate at temperatures from 20°C to 450°C and at pressures from 10^{-6} Torr to 15 atm. The cell is cylindrical with an internal diameter of 3.6 cm capable of accommodating the optical resonator and various diagnostic probes. Additional side tubes are welded onto the cell for diagnostic purposes, and gas access and all ports are sealed by conflat type vacuum flanges using copper gaskets. Since the cell volume is relatively small (about 150 cm³), it is practical to experiment with high pressures of expensive gases such as xenon and to achieve uniform elevated temperature conditions. The cell design permits positioning of the optical resonator axis as close as possible to the electron beam anode foil in order to obtain optimum electron beam energy deposition in the active medium. The distance of the intracell optical resonator axis to a thin titanium foil, which serves as both the anode and pressure barrier between the cell and the electron beam diode, is only 1.6 cm for a resonator of 2.6-cm o.d. The best compromise of electron beam transmission, beam quality, and foil lifetime for the several types and thicknesses of foil used is a 76- μ m thick titanium foil. This foil is supported against cell pressure by a stainless steel grid structure shown in Fig. 2(b). For optical access at high temperatures and pressures, the window design shown in Fig. 2(c) is employed. A sapphire or quartz window flat is sealed to a vacuum flange using a gold wire gasket. On the other side of the window an asbestos or annealed copper ring is used to distribute the sealing pressure. This window design has been successfully tested up to 450°C and 15 atm.

For experiments at elevated temperatures the cell assembly is surrounded by an oven which has ports for

G. Marowsky is with Max-Planck-Institut für Biophysikalische Chemie D-3400 Göttingen, Federal Republic of Germany; the other authors are with Rice University, Electrical Engineering Department, Houston, Texas 77001.

Received 18 February 1978.

0003-6935/78/1101-3491\$0.50/0.

© 1978 Optical Society of America.

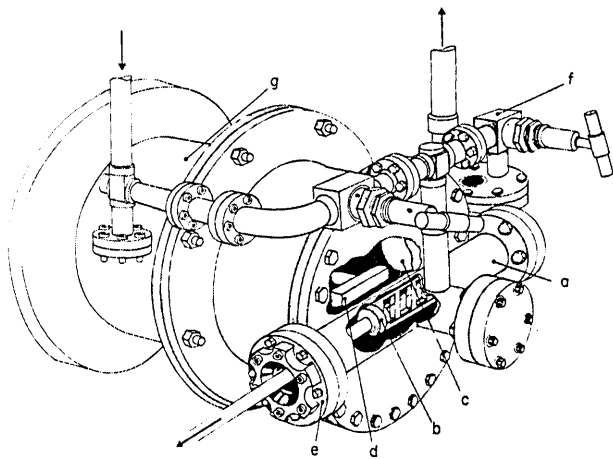


Fig. 1. Illustration of high-temperature high-pressure cell showing (a) reaction cell, (b) optical resonator, (c) anode foil, (d) cathode, (e) optical window, (f) gas handling system, and (g) adaptor flange to electron beam accelerator.

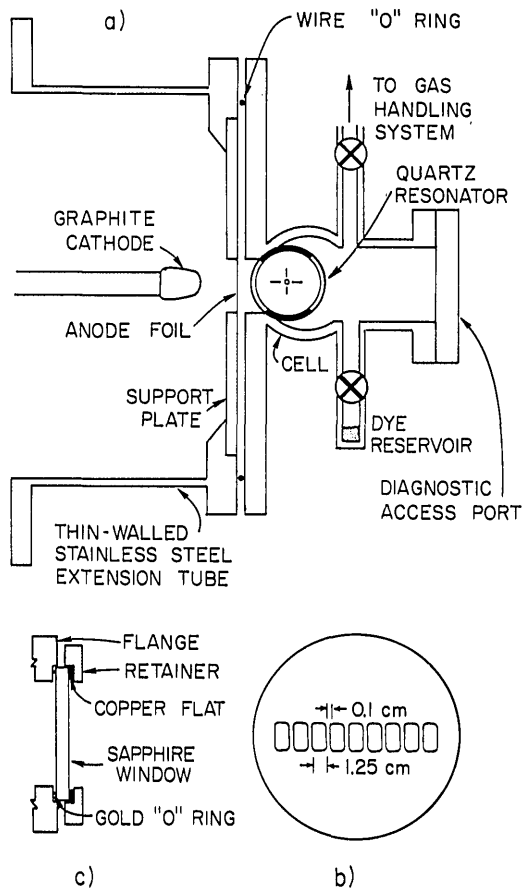


Fig. 2. (a) Cross-sectional view of cell, mounting flange, foil seal, and support plate, and thin-walled stainless steel extension tube for thermal isolation from electron beam machine. The electron beam cathode on its coaxial extension is also shown. (b) Detail of the foil support plate. The thickness of the plate is 0.3 cm. (c) Cross section of high-pressure optical window assembly.

optical access and external vacuum valve operation. Heaters are also clamped to the face plate of the cell and to the windows, providing additional thermal control to insure a temperature distribution. In order to maintain high purity conditions in the reaction cell a separate reservoir chamber is provided which contains the organic or inorganic laser materials to be studied. This provision permitted convenient repetitive refilling of the cell after every complete evacuation cycle to 10^{-6} Torr in order to avoid contamination of both cell and active medium by unwanted reaction products such as organic dye fragments produced by intense electron beam excitation. Thermocouples monitor the slightly higher reservoir temperature and the reaction cell temperature at four separate points. The temperature profile inside the cell can be maintained to $\pm 1^\circ\text{C}$ by controlling the power to each of three heating circuits. Approximately 1 kW is required to maintain a constant temperature of 350°C . In order to achieve an acceptable temperature profile with reasonable power dissipation, it was necessary to isolate thermally the cell assembly from the potentially large heat load of the electron beam accelerator. To achieve this isolation, the cell is mounted on a thin-walled stainless steel extension tube of the electron beam diode chamber [shown in Fig. 1 as part (g)]. The extension tube does not significantly change the electron beam pulse characteristics of the Pulserad 110. The cell assembly is sealed to the foil and extension tube flange as shown in Fig. 2(a), using an 18-gauge welded copper wire gasket. This seal permits a vacuum of 10^{-6} Torr on the diode side and pressures of up to 15 atm inside the cell. It is relatively straightforward to adapt this design of the cell assembly for electron beam pumping using other accelerators. For example, the cell has been coupled to a Systems, Science and Software model Apex I electron beam machine. Although of similar design to the Pulserad 110, this machine can deliver somewhat higher currents, with a longer pulse length. A simple adaptor flange was all that was necessary for mounting the cell. In this case thermal isolation is achieved using either a pressure-controlled drift tube or two thin titanium foils separated by 0.3 cm. One foil serves as the primary anode and pressure barrier, while the second acts as the thermal isolator that minimizes deposition of the hot active medium on the cold primary anode foil.

To simplify the study of a large number of potential buffer gases, a versatile gas handling system was constructed which is capable of evacuating the cell to 10^{-6} Torr and filling it from a manifold that can supply up to eight different gases. Electronic and mechanical gauges monitor the system pressure from 10^{-6} Torr to 15 atm. Since hot vapors would diffuse from the cell and condense on cold regions of the gas system and thus deplete the vapor source, the cell is sealed off within the oven by externally operated all-welded bellows valves. A liquid nitrogen trap is used to condense the vapor when the cell gases are changed.

Optical gain measurements can be made by comparing the intensities of the emitted light from different lengths of the active medium.⁸ By translating an in-

tracell cylindrical aluminum beam shutter that contains a magnet along the axis of the cell by an external magnet, the active length can be conveniently changed. Both magnets are made of Sm-Co alloy, which has a Curie temperature above the cell operating temperature. The shutter contacts stops at either end of its travel so that it moves a known distance.

The cell as described so far can be used very effectively to study the fluorescence and gain of high-temperature laser candidates. To increase the sensitivity of gain measurements and to enhance the electron beam excited population inversion, two types of intracell optical resonators have been designed and evaluated. Both designs utilize two dielectrically coated mirrors attached to a quartz spacer in such a way that resonator alignment is maintained at high temperatures. The quartz mirror substrates may be fused to the spacers without stress caused by mismatched thermal expansion coefficients using a thin pure borosilicate glass transfer tape with a low thermal expansion coefficient. This method may be used at temperatures up to 450°C, but beyond that temperature, the tape begins to anneal at 495°C and soften at 720°C. Even higher operating temperatures may be achieved by sintering the mirror quartz substrates directly to the spacer. This requires a complicated baking procedure up to 950°C. Both of these techniques result in high-quality well-aligned seals. An illustration of the resonator with its optical axis and electron beam input indicated is shown in Fig. 3. Figure 4 shows an interferogram taken under He-Ne laser illumination for a resonator composed of a pair of mirrors ($R = 80\%$) fused by the borosilicate glass tape method to a 7-cm quartz spacer with polished parallel and flat ends. The resolution of two adjacent axial laser modes separated by 600 MHz clearly demonstrates the high optical quality of the prealigned solid quartz resonator. The high temperatures experienced by the resonator reflectors, especially when using the sealant free sintering, required the development of special electron beam deposited dielectric coatings.⁹ Since the reflectance band of a dielectric coating shifts irreversibly to shorter wavelengths upon baking to 950°C for 2 h, the reflective coating design for a specific wavelength region must compensate for this shift. The spectral characteristics before and after baking to elevated temperatures are shown in Fig. 5 for a mirror of 96% reflectivity designed for use with the dye POPOP. A reflectance band shift of about 40 nm toward shorter wavelengths upon baking is clearly evident.

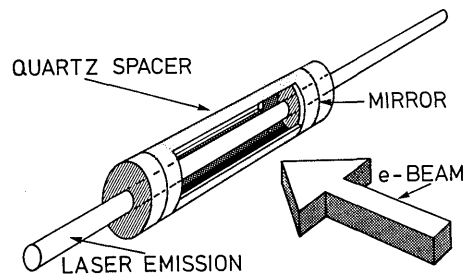


Fig. 3. High-temperature quartz optical resonator assembly.

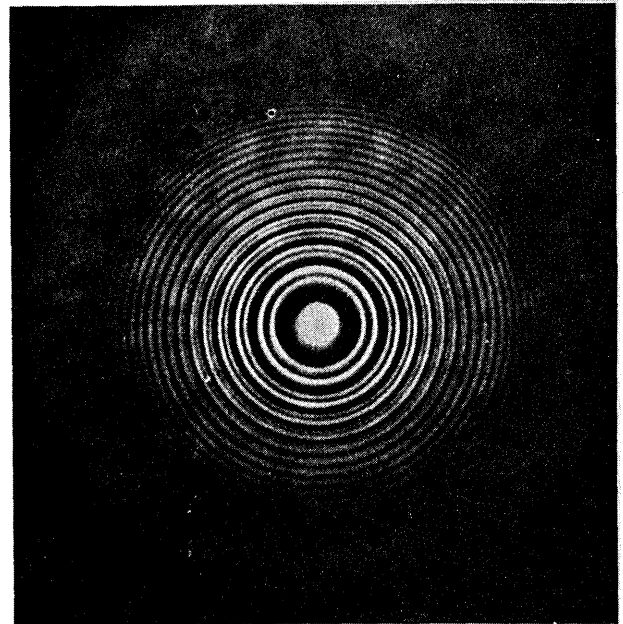


Fig. 4. Interferogram of quartz optical resonator obtained with He-Ne laser illumination. Two axial modes (mode separation ~ 600 MHz) appear well resolved.

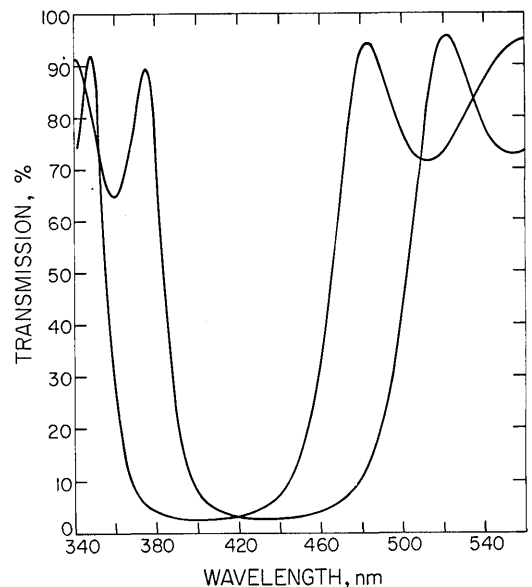


Fig. 5. Room temperature and elevated temperature wavelength characteristics of multilayer dielectric resonator mirrors.

III. Electron Beam Diagnostics and Cell Optimization

As an example of the optimization of electron beam coupling into the cell, we describe the procedures employed in attaching the cell assembly to the Pulserad 110 electron beam accelerator. Such an accelerator typically produces a beam of 1-MeV electrons with a peak current of 15 kA in a 15-nsec pulse. This corresponds to a pulse energy of about 100 J or 15 GW peak power. The diode accelerating voltage is monitored with an oil-insulated resistive voltage divider, and the beam current is measured with a Rogowski coil detector surrounding the diode. By careful optimization of the

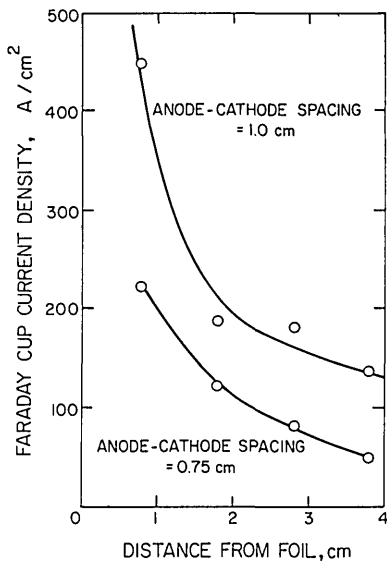


Fig. 6. Current density as a function of the distance between the foil and the Faraday cup. The cathode-anode spacing is used as a parameter. The cell was pressurized with 2 atm of Ar.

graphite cathode shape, its length, and its distance from the anode foil, it is possible to achieve a tight linear electron beam profile and maintain a satisfactory impedance match between diode and the Blumlein pulse discharge network of the accelerator. For a 76- μm thick titanium foil, up to 80% of beam current can be transmitted into the cell. Optimization of intracell current densities and energy was carried out with a Faraday cup type current probe and a segmented calorimeter. Both diagnostic probes could be positioned at various distances from the anode foil. In Fig. 6 the intracell electron beam current density is plotted as a function of the distance from the Faraday cup probe to the anode foil for two anode-cathode spacings, 1 cm and 0.75 cm, at fixed buffer gas pressure and cathode size ($6.4 \times 1.2 \text{ cm}^2$). From Fig. 6 it is apparent that the current density decreases very rapidly from about 0.8 kA/cm² adjacent to the foil to 0.2 kA/cm² at the closest mechanical possible distance of the resonator axis from the foil of about 1.6 cm. Furthermore, it is evident that a reduction of the anode-cathode spacing from 1 cm to 0.75 cm significantly reduces the current density because of a severe diode impedance mismatch. Calorimetric measurements of energy deposited inside the cell confirmed Faraday cup measurements. On the basis of these measurements a cathode-anode spacing of 1 cm for a $6.4 \times 1.5 \text{ cm}^2$ cathode was selected as optimum. Longer and shorter cathodes were also tried and found to give decreased or increased current densities, respectively, but the optimum cathode-anode spacing remained about 1 cm. Decreasing the cathode width did not increase the current density significantly, probably because of increased electron emission off the sides and beam defocusing. Additional electron beam propagation studies inside the cell were performed using thermally sensitive sheets of plastic film¹⁰ supported

on titanium or aluminum sheets. An evaluation of the intracell electron beam profile by this method indicates that the incident rectangular cross section adjacent to the anode foil changes to a circular cross section after the beam has propagated several centimeters beyond the anode.

IV. High-Temperature Optical Gain Studies

The merits of the cell and the resonator described above have been evaluated in several ways. Several buffer gases and gas mixtures were used over a wide range of buffer gas pressures and dye vapor partial pressures, determined by cell temperature, in an effort to determine the best combination for an electron beam excited dye vapor laser. Gain measurements on Ar-N₂ and Ar-buffered POPOP dye vapor have been made, and a study of the temperature dependence of the Ar-N₂ laser mixtures optical gain was measured by means of a continuous variation of the electron beam pumped active length. In the case of the dye POPOP gain was determined by comparison of the fluorescence intensity of 3-cm and 6-cm excited active length. Details of such gain measurements are reported in Refs. 8, 11, and 12. Successful application of this method requires uniform excitation of the entire active medium, a condition that does not always exist for transverse electron beam excitation. Alternatively, gain can be measured by probing the fluorescence from the entire pumped active medium either from a single or double pathlength¹³ that can be established by alignment of a magnetically operated intracell reflector.

The results of a series of gain measurements of a 10% Ar-N₂ mixture at room temperature and total pressure of 3 atm are shown in Fig. 7. The dashed line corresponds to the recorded fluorescence as a function of the active region length. For a short active region ($x < 3 \text{ cm}$), the experimental results can be fitted to an exponential function characterized by an unsaturated net gain of 0.6 cm^{-1} , as depicted by the solid line in Fig. 7.

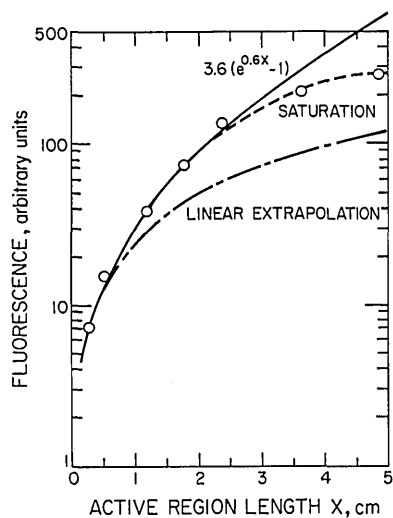


Fig. 7. Fluorescence output from a premixed 10% nitrogen in Ar mixture, as a function of the length of the active region. The solid line is a fit to data obtained with the expression $I = I_0/\alpha(e^{\alpha x} - 1)$.

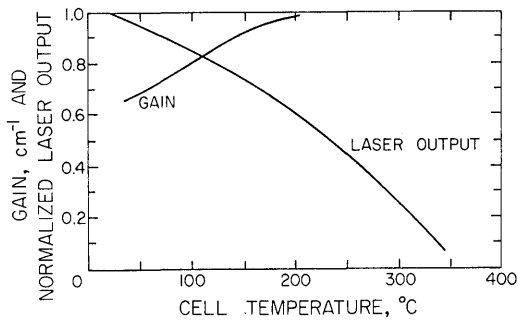


Fig. 8. Gain and normalized laser output power for Ar-N₂ as a function of temperature. The gain is in cm⁻¹, while the laser output is normalized to the output at room temperature (25°C).

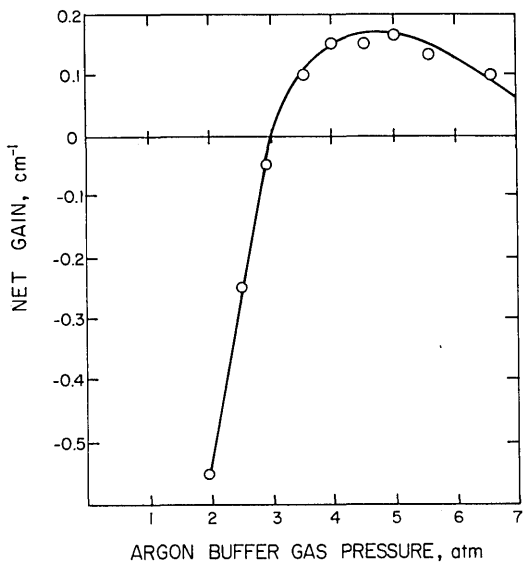


Fig. 9. Gain of POPOP dye vapor at 1 Torr partial pressure as a function of Ar pressure.

For an active region, where $x > 3$ cm, the Ar-N₂ fluorescence exhibits increasing saturation. For comparison, the zero gain situation is shown as a linear extrapolation by the interrupted line in Fig. 7. Hence reliable Ar-N₂ gain data can only be obtained by comparing the fluorescence of 1-cm and 2-cm electron beam pumped active lengths. This procedure has been successfully applied to measure the gain of such a laser mixture at elevated temperatures as plotted in Fig. 8. The Ar-N₂ gain is seen to increase slightly with increasing temperature from 0.6 cm⁻¹ at room temperature to almost 1 cm⁻¹ at 250°C. It should be noted that although the output from the laser decreases significantly, the gain remains quite high. We believe this situation arises from a temperature dependent competition mechanism within the Ar reaction channel. As the temperature increases, energy delivered to the Ar from the electron

beam is diverted away from the important nitrogen pumping. This reduces the number of excited species, without actually reducing the relative population inversion. Laser action of Ar-N₂ also served to test the alignment stability of the intracell quartz resonator at high temperatures.

The above-described cell assembly has been used, in particular, to examine the gain characteristics of potential electron beam excited laser candidates such as organic dye vapors. Figure 9 depicts the dependence of the small signal gain of POPOP dye at 1 Torr partial pressure (~280°C) upon buffer gas pressure. The data were taken by probing the gain along the optical axis for 3-cm and 6-cm long electron beam excited active regions. At an optimum Ar buffer gas pressure of about 4.5 atm, we were able to obtain up to 0.17 cm⁻¹ gain for POPOP.¹²

The authors are grateful to W. Sauerman for his skillful fabrication of optical resonators and to F. P. Schäfer for his stimulating discussion of the high-temperature optical gain studies.

This work was supported in part by the National Science Foundation, the Robert A. Welch Foundation, the Department of Energy, and NATO.

References

1. S. A. Edelstein, *Opt. Commun.* **21**, 27 (1977).
2. G. Marowsky, R. Cordray, F. Tittel, B. Wilson, and J. W. Keto, *J. Chem. Phys.* **67**, 4845 (1977).
3. C. T. Ryan and T. K. Gustafson, *Chem. Phys. Lett.* **44**, 241 (1976).
4. J. Kofflend, R. W. Field, D. R. Guyer, and S. R. Leone, *Laser Spectroscopy III*, J. Hall and J. L. Carlsten, Eds. (Springer, Berlin, 1977), p. 382.
5. R. R. Jacobs and W. F. Krupke, *Electronic Transition Lasers*, L. E. Wilson, S. N. Surchard, and J. F. Steinfield, Eds. (MIT Press, Cambridge, 1977), p. 246; also *Appl. Phys. Lett.* **32**, 31 (1978).
6. C. Rhodes, R. R. Jacobs, and L. Schlie, 7th Winter Colloquium on High Power Visible Lasers, Park City, Utah, 16-18 February 1977.
7. J. J. Ewing and C. A. Brau, in *Tunable Lasers and Applications*, A. Mooradian, Ed. (Springer, Berlin, 1976).
8. C. V. Shank, *Rev. Mod. Phys.* **47**, 649 (1975).
9. Developed in cooperation with M. Houben, Perkin-Elmer Corporation, Norwalk, Conn.
10. 3M transparency film, ir sensitive, type 529.
11. G. Marowsky, R. Cordray, F. K. Tittel, W. Wilson, and C. B. Collins, submitted to *IEEE J. Quantum Electron.* **QE-14**, 434 (1978).
12. G. Marowsky, R. Cordray, F. K. Tittel, and W. L. Wilson, accepted by *Appl. Phys. Lett.* **32**, 561 (1978).
13. M. L. Bhaumik, *Inst. Phys. Conf. Ser.* **29**, 122 (1976).